



# Electronic Spectra and Their Relation to the ( , ) Collective Mode in High- Tc Superconductors

著者	Campuzano J. C., Ding H., Norman M. R., Fretwell H. M., Randeria M., Kaminski A., Mesot J., Takeuchi T., Sato T., Yokoya T., Takahashi T., Mochiku T., Kadowaki K., Guptasarma P., Hinks D. G., Konstantinovic Z., Li Z. Z., Raffy H.
journal or publication title	Physical review letters
volume	83
number	18
page range	3709-3712
year	1999-11
権利	(C)1999 The American Physical Society
URL	<a href="http://hdl.handle.net/2241/89215">http://hdl.handle.net/2241/89215</a>

doi: 10.1103/PhysRevLett.83.3709

## Electronic Spectra and Their Relation to the $(\pi, \pi)$ Collective Mode in High- $T_c$ Superconductors

J. C. Campuzano,<sup>1,2</sup> H. Ding,<sup>3</sup> M. R. Norman,<sup>2</sup> H. M. Fretwell,<sup>1</sup> M. Randeria,<sup>4</sup> A. Kaminski,<sup>1</sup> J. Mesot,<sup>2</sup> T. Takeuchi,<sup>5</sup> T. Sato,<sup>6</sup> T. Yokoya,<sup>6</sup> T. Takahashi,<sup>6</sup> T. Mochiku,<sup>7</sup> K. Kadowaki,<sup>8</sup> P. Guptasarma,<sup>2</sup> D. G. Hinks,<sup>2</sup> Z. Konstantinovic,<sup>9</sup> Z. Z. Li,<sup>9</sup> and H. Raffy<sup>9</sup>

<sup>1</sup>*Department of Physics, University of Illinois at Chicago, Chicago, Illinois 60607*

<sup>2</sup>*Materials Sciences Division, Argonne National Laboratory, Argonne, Illinois 60439*

<sup>3</sup>*Department of Physics, Boston College, Chestnut Hill, Massachusetts 02467*

<sup>4</sup>*Tata Institute of Fundamental Research, Mumbai 400005, India*

<sup>5</sup>*Department of Crystalline Materials Science, Nagoya University, Nagoya 464-01, Japan*

<sup>6</sup>*Department of Physics, Tohoku University, 980-8578 Sendai, Japan*

<sup>7</sup>*National Research Institute for Metals, Sengen, Tsukuba, Ibaraki 305, Japan*

<sup>8</sup>*Institute of Materials Science, University of Tsukuba, Ibaraki 305, Japan*

<sup>9</sup>*Laboratoire de Physique des Solides, Université de Paris-Sud, 91405 Orsay Cedex, France*

(Received 22 June 1999)

The photoemission line shape near  $(\pi, 0)$  in  $\text{Bi}_2\text{Sr}_2\text{CaCu}_2\text{O}_{8+\delta}$  below  $T_c$  is characterized by a sharp peak, followed at higher energy by a dip and hump. We study the evolution of this line shape as a function of momentum, temperature, and doping. We find the hump scales with the peak and persists above  $T_c$  in the pseudogap state. We present strong evidence that the peak-dip-hump structure arises from the interaction of electrons with a collective mode of wave vector  $(\pi, \pi)$ . The inferred mode energy and its doping dependence agree well with a magnetic resonance observed by neutron scattering.

PACS numbers: 74.25.Jb, 71.18.+y, 74.72.Hs, 79.60.Bm

In the high temperature copper oxide superconductors, a small change in doping takes the material from an antiferromagnetic insulator to a  $d$ -wave superconductor. This raises the fundamental question of the relation of the electronic structure of the doped superconductor [1] to that of the parent insulator [2]. Here we examine this by using angle resolved photoemission spectroscopy (ARPES). We find that the spectra in the superconducting state near the  $(\pi, 0)$  point of the Brillouin zone are composed of two distinct features (the peak and the hump), precursors of which exist in the pseudogap state (the low energy and high energy pseudogaps). Their evolution and dispersion as a function of doping can be understood as arising from the interaction of the electrons with a collective mode [3,4] which has the same  $(\pi, \pi)$  wave vector characteristic of the magnetic insulator, and whose energy decreases as the doping is reduced. This is supported by our observation that the mode energy inferred from ARPES as a function of doping correlates strongly with that obtained directly from neutron scattering data [5], and points to the intimate relation of magnetic correlations to high  $T_c$  superconductivity.

The experiments were carried out using procedures and samples described previously [6], as well as films grown by rf magnetron sputtering [7]. The doping level was controlled by varying oxygen stoichiometry, with samples labeled by their onset  $T_c$ . Spectra were obtained with a photon energy of 22 eV and a photon polarization directed along the CuO bond direction. Spectra had energy resolutions (FWHM) of 17, 26, or 34 meV with a momentum window of radius  $0.045\pi/a$ . Energies

are measured with respect to the chemical potential, determined using a polycrystalline Pt or Au reference in electrical contact with the sample.

We begin with the  $T$  evolution of the spectra of  $\text{Bi}_2\text{Sr}_2\text{CaCu}_2\text{O}_{8+\delta}$  (Bi2212) near the  $(\pi, 0)$  point of the Brillouin zone (inset of Fig. 1a). In the underdoped region of the phase diagram (that lies between the undoped insulator and optimal doping, corresponding to the highest  $T_c$ ), one observes a pseudogap (30–50 meV) which is very likely associated with pairing above  $T_c$ , a precursor to superconductivity [6,8]. For temperatures above the pseudogap temperature scale  $T^*$  [6] we see a broad peak which is chopped off by the Fermi function, as shown in Fig. 1a for an underdoped 83 K sample at 200 K. In this respect, the one-particle spectral function of the underdoped compounds, which is completely incoherent, is similar to that observed in the overdoped compounds. While there is only weak dispersion from  $(\pi, 0) \rightarrow (\pi, \pi)$  for  $T > T^*$ , there is definite loss of integrated spectral weight [9], and one can identify the  $(\pi, 0) \rightarrow (\pi, \pi)$  “Fermi surface” crossing [10].

As the temperature is reduced below  $T^*$ , but still above  $T_c$ , we see that the spectral function remains completely incoherent, as shown in Fig. 1b for an underdoped 89 K sample. The leading edge pseudogap [6,8] which develops below  $T^*$  is difficult to see on the energy scale of Fig. 1b (the midpoint shift at 135 K is 3 meV). However, a higher energy feature (the “high energy pseudogap”) can easily be identified by a change in slope of the spectra as a function of energy (see Fig. 2). On further reduction of the temperature below  $T_c$ , a coherent quasiparticle peak

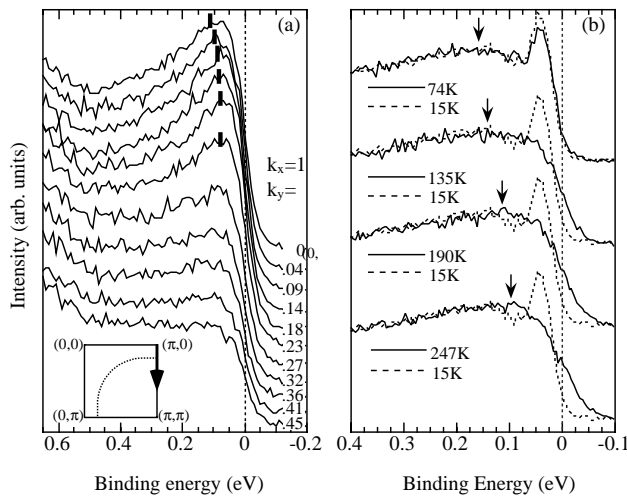


FIG. 1. Dispersion and temperature dependence of spectra near  $(\pi, 0)$ : (a) Spectra along  $(\pi, 0) \rightarrow (\pi, \pi)$  for an underdoped 83 K sample at 200 K (above  $T^*$ ), with the thick vertical bar indicating the peak position. The curves are labeled in units of  $\pi/a$ . The Brillouin zone is shown as an inset, with the Fermi surface as a dotted line. (b) Temperature evolution of the spectra at the  $(\pi, 0)$  point for an underdoped 89 K sample, with the positions of the high energy feature marked by arrows.

begins to grow at the position of the leading edge gap, accompanied by a redistribution of the incoherent spectral weight leading to a dip and hump structure [9,11]. The peak-dip-hump line shape and the dispersion of these features will play a central role in our discussion.

The high energy pseudogap feature is closely related to the hump below  $T_c$ , as seen from a comparison of their dispersions. We show data along  $(\pi, 0) \rightarrow (\pi, \pi)$

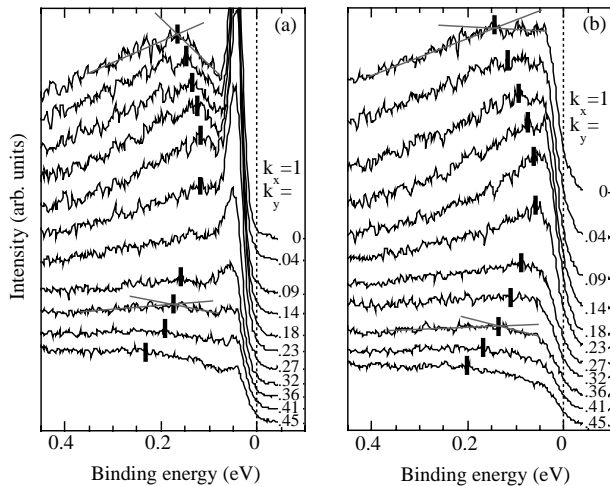


FIG. 2. Spectra along  $(\pi, 0) \rightarrow (\pi, \pi)$  in (a) the superconducting state ( $T = 60$  K), and (b) the pseudogap state ( $T = 100$  K) for an underdoped 75 K sample (curves are labeled in units of  $\pi/a$ ). The thick vertical bar indicates the position of the higher energy feature, at which the spectrum changes slope as highlighted by the intersecting straight lines.

for an underdoped 75 K sample in the superconducting state (Fig. 2a) and in the pseudogap regime (Fig. 2b). Below  $T_c$ , the sharp peak at low energy is essentially dispersionless, while the higher energy hump rapidly disperses from the  $(\pi, 0)$  point towards the  $(\pi, 0) \rightarrow (\pi, \pi)$  Fermi crossing [10] seen above  $T^*$ . Beyond this, the intensity drops dramatically, but there is clear evidence that the hump disperses back to higher energy. In the pseudogap state, the high energy feature also shows strong dispersion [8,12], much like the hump below  $T_c$ , even though the leading edge is nondispersive like the sharp peak in the superconducting state.

In Fig. 3 we show the dispersion of the sharp peak and hump (below  $T_c$ ), for a variety of doping levels, in the vicinity of the  $(\pi, 0)$  point along the two principal axes. The sharp peak at low energies is seen to be essentially nondispersive along both directions for all doping levels, while the hump shows very interesting dispersion. Along  $(\pi, 0) \rightarrow (0, 0)$  (Fig. 3a), the hump exhibits a maximum, with an eventual dispersion away from the Fermi energy, becoming rapidly equivalent to the binding energy of the broad peak in the normal state as one moves away from the region near  $(\pi, 0)$  [13]. In the orthogonal direction (Fig. 3b), since the hump initially disperses towards the  $(\pi, 0) \rightarrow (\pi, \pi)$  Fermi crossing, which is known to be a weak function of doping [10], one obtains the rather dramatic effect that the dispersion becomes stronger with underdoping. We also note that there is an energy separation between the peak and the hump due to the spectral dip. In essence, the hump disperses towards the spectral dip, but cannot cross it, with its weight dropping strongly as the dip energy is approached. Beyond this point, one sees evidence of the dispersion bending back to higher binding energy for more underdoped samples.

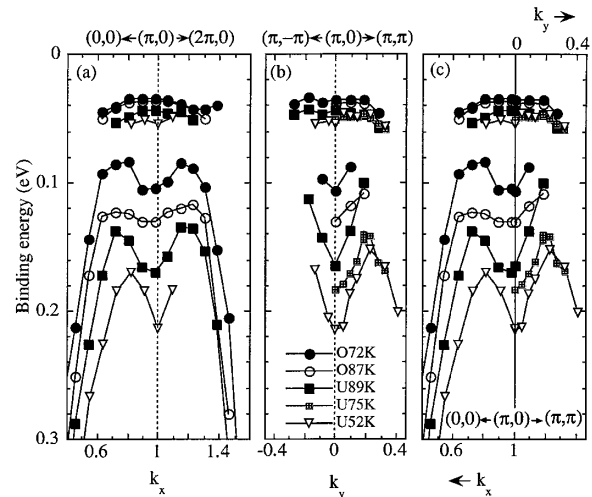


FIG. 3. Doping dependence of the dispersion from (a)  $(\pi, 0) \rightarrow (\pi \pm \pi, 0)$ , (b)  $(\pi, 0) \rightarrow (\pi, \pm \pi)$ , and (c) both directions, for the peak and hump in the superconducting state. U is underdoped and O is overdoped. Points were obtained by polynomial fits to the data, and are consistent with the simpler criterion used in Fig. 2.

Figure 4a shows the evolution of the low temperature spectra at the  $(\pi, 0)$  point as a function of doping. The sharp quasiparticle peak moves to higher energy, indicating that the gap increases with underdoping [14] (although this is difficult to see on the scale of Fig. 4a). We see that the hump moves rapidly to higher energy with underdoping [15]. These trends can be seen very clearly in Fig. 4b, where the energy of the peak and hump are shown as a function of doping for a large number of samples. Finally, we observe that the quasiparticle peak loses spectral weight with increasing underdoping, as expected for a doped Mott insulator; in addition, the hump also loses spectral weight, though less rapidly.

The hump below  $T_c$  is clearly related to the superconducting gap, given the weak doping dependence of the ratio between the hump and quasiparticle peak positions at  $(\pi, 0)$ , shown in Fig. 4c. Tunneling data find this same correlation on a wide variety of high- $T_c$  materials whose energy gaps vary by a factor of 30 [16]. We have additional strong evidence [1,13] that the peak and hump do *not* arise from two different “bands.”

Thus, the peak, dip, and hump are features of a single spectral function, and imply a strong frequency dependence of the superconducting state self-energy (a “strong-coupling effect”). The hump represents the energy scale at which the spectral function below  $T_c$  matches onto that in the normal state (as evident from the data in the bottom curve of Fig. 1b). However, the existence of the dip requires additional structure in the self-energy. We had suggested that this structure can be naturally understood in terms of electrons interacting with a sharp collective mode [13,17] below  $T_c$ , which also leads to an explana-

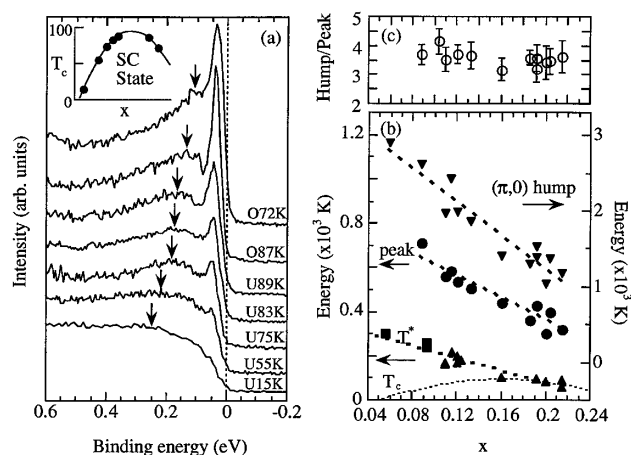


FIG. 4. Dependence of energy scale on carrier density: (a) Doping dependence of the spectra ( $T = 15$  K) at the  $(\pi, 0)$  point (U55K is a film). The inset shows  $T_c$  vs doping. (b) Doping dependence of  $T_c^*$ , and the peak and hump binding energies in the superconducting state along with their ratio (c), as a function of doping,  $x$ . The empirical relation between  $T_c$  and  $x$  is given by  $T_c/T_c^{\max} = 1 - 82.6(x - 0.16)^2$  [25] with  $T_c^{\max} = 95$  K. For  $T_c^*$ , solid squares represent lower bounds.

tion of the nontrivial dispersion, as discussed below. It was speculated that the mode was the same as that observed directly by neutron scattering in  $\text{YBa}_2\text{Cu}_3\text{O}_7$  [3,4], and more recently in Bi2212 [18,19].

To motivate the analysis below that firmly establishes the mode interpretation of ARPES spectra and its connection with neutron data, we need to recall [13,17] that the spectral dip represents a pairing induced gap in the incoherent part of the spectral function at  $(\pi, 0)$  occurring at an energy  $\Delta + \Omega_0$ , where  $\Delta$  is the superconducting gap and  $\Omega_0$  is the mode energy. We can estimate the mode energy from ARPES data from the energy difference between the dip ( $\Delta + \Omega_0$ ) and the quasiparticle peak ( $\Delta$ ).

In Fig. 5b we plot the mode energy as estimated from ARPES for various doping levels as a function of  $T_c$  and compare it with neutron measurements. We find striking agreement both in terms of the energy scale and its doping dependence [5]. We note that the mode energy inferred from ARPES decreases with doping, just like the neutron data, unlike the gap energy (Fig. 4b), which increases. This can be seen directly in the raw data, shown in Fig. 5a. Moreover, there is strong correlation between the temperature dependences in the ARPES and neutron data. While neutrons see a sharp mode only below  $T_c$ , a smeared out remnant persists up to  $T^*$  [20]. As the sharpness of the mode is responsible for the sharp spectral dip, one then sees the correlation with ARPES where the dip disappears above  $T_c$ , but with a remnant of the hump persisting to  $T^*$ .

An important feature of the neutron data is that the mode exists only in a narrow momentum range about  $(\pi, \pi)$  and is magnetic in origin [4]. To see a further connection with ARPES, we return to the results of Fig. 3. Note the dispersion along the two orthogonal directions are similar (Fig. 3c), unlike the dispersion inferred in the

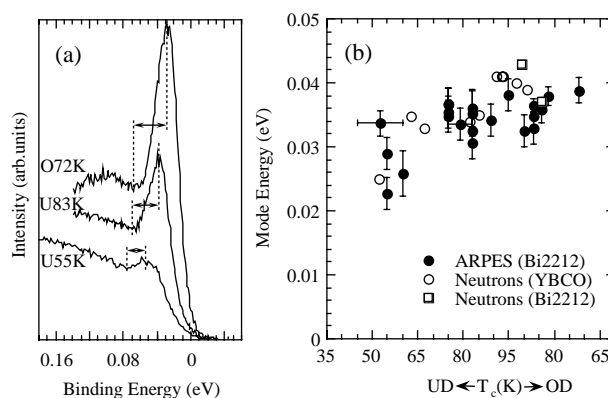


FIG. 5. Doping dependence of the mode energy: (a) Spectra at  $(\pi, 0)$  showing the decrease in the energy separation of the peak and dip with underdoping. Peak and dip locations were obtained by independent polynomial fits and carefully checked for the effects of energy resolution. (b) Doping dependence of the collective mode energy inferred from ARPES together with that inferred from neutron data (for the latter, YBCO results as compiled in Ref. [5], Bi2212 results of Refs. [18] and [19]).

normal state [1]. As these two directions are related by a  $(\pi, \pi)$  translation  $[(x, 0) \equiv (0, -x); (0, -x) + (\pi, \pi) = (\pi, \pi - x)]$ , we see that the hump dispersion is clearly reflecting the  $(\pi, \pi)$  nature of the collective mode. This dispersion is also consistent with a number of models [21,22] in the literature which identify the high energy feature in the pseudogap regime as a remnant of the insulating magnet. We note, though, that the mode is due to quasiparticle pair creation and thus not just a continuation of the spin wave mode from the antiferromagnet [23].

This brings up a question that is at the heart of the high  $T_c$  problem: how can a feature which can be understood as a strong-coupling effect of superconductivity, as discussed above, turn out to have a dispersion that resembles that of a magnetic insulator? The reason is that the collective mode has the same wave vector,  $(\pi, \pi)$ , which characterizes the magnetic order of the insulator. It is easy to demonstrate that in the limit that the mode energy goes to zero (long range order), one actually reproduces a symmetric dispersion similar to that in Fig. 3c, with the spectral gap determined by the strength of the mode [21]. This is in accord with the increase in the hump energy with underdoping (Fig. 4b) tracking the rise in the neutron mode intensity [5]. Since the hump scales with the superconducting gap, the obvious implication is that the mode is intimately connected with pairing, a conclusion which can also be made by relating the mode to the superconducting condensation energy [24]. That is, high  $T_c$  superconductivity is likely due to the same magnetic correlations which characterize the insulator and give rise to the mode.

This work was supported by the National Science Foundation DMR 9624048, and DMR 91-20000 through the Science and Technology Center for Superconductivity, the U.S. Dept. of Energy, Basic Energy Sciences, under Contract No. W-31-109-ENG-38, the CREST of JST, and the Ministry of Education, Science, and Culture of Japan. The Synchrotron Radiation Center is supported by NSF DMR 9212658. J.M. is supported by the Swiss National Science Foundation, and M.R. by the Swarnajayanti fellowship of the Indian DST.

- [1] H. Ding *et al.*, Phys. Rev. Lett. **76**, 1533 (1996).
- [2] B.O. Wells *et al.*, Phys. Rev. Lett. **74**, 964 (1995); F. Ronning *et al.*, Science **282**, 2067 (1998).
- [3] J. Rossat-Mignod *et al.*, Physica (Amsterdam) **185-189C**, 86 (1991).
- [4] H. A. Mook *et al.*, Phys. Rev. Lett. **70**, 3490 (1993); H. F. Fong *et al.*, *ibid.* **75**, 316 (1995).
- [5] Neutron results are reviewed by P. Bourges, in *The Gap Symmetry and Fluctuations in High  $T_c$  Superconductors*, edited by J. Bok *et al.* (Plenum, New York, 1998), p. 349.
- [6] H. Ding *et al.*, Nature (London) **382**, 51 (1996).
- [7] Z. Konstantinovic, Z.Z. Li, and H. Raffy, Physica (Amsterdam) **259-261B**, 567 (1999).
- [8] D. S. Marshall *et al.*, Phys. Rev. Lett. **76**, 4841 (1996).
- [9] M. Randeria *et al.*, Phys. Rev. Lett. **74**, 4951 (1995).
- [10] H. Ding *et al.*, Phys. Rev. Lett. **78**, 2628 (1997).
- [11] D. S. Dessau *et al.*, Phys. Rev. Lett. **66**, 2160 (1991).
- [12] P.J. White *et al.*, Phys. Rev. B **54**, R15 669 (1996).
- [13] M.R. Norman *et al.*, Phys. Rev. Lett. **79**, 3506 (1997).
- [14] J.M. Harris *et al.*, Phys. Rev. B **54**, R15 665 (1996); H. Ding *et al.*, J. Phys. Chem. Solids **59**, 1888 (1998).
- [15] R. B. Laughlin, Phys. Rev. Lett. **79**, 1726 (1997).
- [16] J. Zasadzinski *et al.*, Proc. SPIE Int. Soc. Opt. Eng. **2696**, 338 (1996); N. Miyakawa *et al.*, Phys. Rev. Lett. **83**, 1018 (1999).
- [17] M.R. Norman and H. Ding, Phys. Rev. B **57**, R11 089 (1998).
- [18] H. A. Mook, F. Dogan, and B.C. Chakoumakos, e-print cond-mat/9811100.
- [19] H. F. Fong *et al.*, Nature (London) **398**, 588 (1999).
- [20] P. Dai *et al.*, Phys. Rev. Lett. **77**, 5425 (1996).
- [21] A. P. Kampf and J.R. Schrieffer, Phys. Rev. B **42**, 7967 (1990).
- [22] R. Preuss, W. Hanke, C. Grober, and H.G. Evertz, Phys. Rev. Lett. **79**, 1122 (1997); J. Schmalian, D. Pines, and B. Stojkovic, *ibid.* **80**, 3839 (1998); X.-G. Wen and P. A. Lee, *ibid.* **76**, 503 (1996); Z.-X. Shen and J.R. Schrieffer, *ibid.* **78**, 1771 (1997).
- [23] E. Demler and S.-C. Zhang, Phys. Rev. Lett. **75**, 4126 (1995).
- [24] E. Demler and S.-C. Zhang, Nature (London) **396**, 733 (1998); P. Dai *et al.*, Science **284**, 1344 (1999).
- [25] M.R. Presland *et al.*, Physica (Amsterdam) **176C**, 95 (1991).